



Full length article

## Visible-light-induced self-cleaning functional fabrics using graphene oxide/carbon nitride materials

Marta Pedrosa<sup>a</sup>, Maria J. Sampaio<sup>a,\*</sup>, Tajana Horvat<sup>a</sup>, Olga C. Nunes<sup>b</sup>, Goran Dražić<sup>c</sup>,  
Alírio E. Rodrigues<sup>a</sup>, José L. Figueiredo<sup>a</sup>, Cláudia G. Silva<sup>a</sup>, Adrián M.T. Silva<sup>a</sup>, Joaquim L. Faria<sup>a</sup>

<sup>a</sup> Laboratory of Separation and Reaction Engineering - Laboratory of Catalysis and Materials (LSRE-LCM), Faculty of Engineering, University of Porto, Rua Dr. Roberto Frias, 4200-465 Porto, Portugal

<sup>b</sup> LEPAE – Chemical Engineering Department, Faculty of Engineering, University of Porto, Porto 4200-465, Portugal

<sup>c</sup> Department of Materials Chemistry, National Institute of Chemistry, Ljubljana 1000, Slovenia

### ARTICLE INFO

#### Keywords:

Photocatalysis  
Carbon nanostructures  
Cotton  
Decontamination  
Disinfection

### ABSTRACT

Functional cotton fabrics consisting of neat polymeric carbon nitride (CN) combined with graphene oxide (GO) were prepared by a simple impregnation route. The CN-based coated fabrics were characterized by several techniques. The self-cleaning efficiency of these hybrid fabrics was assessed in the photocatalytic degradation of caffeine and rhodamine B (RhB) in aqueous solutions under visible light-emitting diodes (LEDs). It was demonstrated that GO, even if present at a low % v/v (0.1%), confers to the coated fabrics higher photocatalytic efficiency for degradation of both organic pollutants in comparison with CN coated fabrics. The photoluminescence quenching observed on coated GO/CN fabrics suggests an electron transfer between the CN and GO phases. In general, both coated CN and GO/CN fabrics show high stability after three uses with intensive washes between each run. The antibacterial activity against *Escherichia coli* using CN and GO/CN colloids was assessed. Results showed > 99.2% of *E. coli* inactivation with CN-based colloids activated by visible radiation.

### 1. Introduction

The growing concern about the generalized environmental pollution and its side effects on human health has been attracting the attention of both scientific and industrial communities. The development of functional fabrics that can reduce/eliminate organic compounds and pathogenic microorganisms may constitute a step-forward to improve and sustain human and environmental well-being. Coatings with anti-odor, photocatalytic self-cleaning, UV-protection, hydrophobicity, and antibacterial properties have been well described in the literature [1–6]. Textile-nanoparticle hybrids have been prepared with a wide range of nanomaterials, such as CuO, CdS, ZnO and TiO<sub>2</sub> [7–10]. Furthermore, the broad-spectrum of Ag nanoparticles boost their extended use in clothing, biomedical applications, cosmetics, water and air treatment, among others [11–15]. Nevertheless, there is still some contradiction in the impregnation of Ag nanoparticles on textiles, due to side effects caused either by their direct contact with the skin, human body absorption and accumulation, as well as their spreading into the environment [16].

The pioneering work of Matsunaga *et al.* [17], reporting the application of heterogeneous photocatalysis for the inactivation of bacteria

using Pt-loaded TiO<sub>2</sub> catalysts, led to the development of photocatalysts with self-cleaning and antimicrobial properties [18,19]. Since metal accumulation is a problem for both humans and the environment, the development of optical semiconductors, which can be safely used and are also economically more attractive than the current market options, has become a priority.

Polymeric graphite-like carbon nitride (g-C<sub>3</sub>N<sub>4</sub>) has received a great deal of attention for photocatalytic applications such as hydrogen production, organic synthesis and pollutants degradation [20–22]. Few recent works have documented the use of g-C<sub>3</sub>N<sub>4</sub> based materials on the preparation of smart functional textiles with self-cleaning properties [5,23,24]. For instance, Fan *et al.* [5] immobilized g-C<sub>3</sub>N<sub>4</sub> nanosheets on cotton fabrics and investigated the photocatalytic removal of red wine and coffee stains using a solar simulator. In another work, smart textiles consisting of metal organic framework/g-C<sub>3</sub>N<sub>4</sub> nanospheres achieved high activity for the detection/detoxification of chemical warfare agents, the carbon nitride nanospheres playing a crucial role in the detoxification function of the fabricated composite [23]. The common main challenge in fabrics functionalization relies on the efficient and durable impregnation of the textiles, to assume minimal activity loss. Thus, an effective cross-linking between the fabrics and the

\* Corresponding author.

E-mail address: [mjsampaio@fe.up.pt](mailto:mjsampaio@fe.up.pt) (M.J. Sampaio).

<https://doi.org/10.1016/j.apsusc.2019.143757>

Received 17 March 2019; Received in revised form 21 June 2019; Accepted 21 August 2019

Available online 22 August 2019

0169-4332/ © 2019 Elsevier B.V. All rights reserved.

catalysts is imperative.

The novelty of the present study relies on the preparation of metal-free photocatalysts based on g-C<sub>3</sub>N<sub>4</sub> and graphene oxide (GO) and their impregnation on cotton fabrics. The self-cleaning ability of the resulting coated fabrics was tested in the photocatalytic degradation of caffeine and RhB under visible LED light radiation, and their stability was assessed. The study was extended to evaluate the photocatalytic efficiency of the nanocarbon materials on *Escherichia coli* inactivation. To the best of our knowledge, this is the first work reporting both self-cleaning and antibacterial performance of g-C<sub>3</sub>N<sub>4</sub>/GO hybrids under visible-LED irradiation.

## 2. Experimental

### 2.1. Materials

Dicyandiamide (DCN, 99%), caffeine ( $\geq 99\%$ ), rhodamine (RhB,  $\geq 95\%$ ), synthetic graphite (particle size  $\leq 2\ \mu\text{m}$ ), sodium nitrate (NaNO<sub>3</sub>, 99%), hydrochloric acid (HCl, 37%) and sulfuric acid (H<sub>2</sub>SO<sub>4</sub>, > 95%) were purchased from Sigma-Aldrich. Hydrogen peroxide (H<sub>2</sub>O<sub>2</sub>, 30% w/v), sodium chloride (NaCl, 99%) and potassium permanganate (KMnO<sub>4</sub>, 99 wt%) were obtained from Fisher, Panreac and Merck, respectively. Mueller-Hinton agar was purchased from Oxoid. Formic acid (98%) and acetonitrile (99.8%) were supplied by Fluka. All solutions were prepared fresh with ultrapure water (UP) obtained with a Direct-Q Milipore system.

### 2.2. Catalysts preparation and cotton functionalization

The synthesis and characterization of the polymeric carbon nitride (CN) and the graphene oxide (GO) have been extensively described in previous works [25,26]. The aqueous colloidal CN used in the present study was prepared by sonication using an ultrasonic processor UP400S 24 kHz. Briefly, a certain amount of CN was added to UP water and sonicated for 50 min. Then, the suspension was centrifuged at 3500 rpm for 15 min and the colloidal CN was recovered. The same procedure was used for the preparation of the colloidal GO/CN. In this case, 0.1% v/v of GO suspension was added to the colloidal CN and mixed for 30 min. The amount of GO suspension employed in this work was selected based on prior studies using 0.5% v/v and 1.0% v/v, which showed lower photocatalytic performance for the degradation of organic compounds compared with 0.1% v/v and neat CN.

Before the colloidal CN or GO/CN coating, uncoated cotton fabrics were exhaustively washed with UP water and anionic detergent for 1 h at 40 °C. Then, the uncoated fabrics were immersed in a certain volume of colloidal CN or GO/CN ( $\sim 0.7\ \text{g L}^{-1}$ ), and heated at 40 °C using a water bath orbital shaker for 3 h. The cotton fabrics were passed through a two roller foulard (Roaches EHP Padder), under 1 bar pressure at speed rate of  $3\ \text{m min}^{-1}$ , followed by a thermal step using a thermofixation chamber (Roaches, Model Mini Thermo) with circulating air at a temperature of 100 °C for 4 min. Then, the functionalized fabrics were washed with UP water at 70 °C to remove some potential photocatalyst particles, which were not anchored to the cotton fabrics. The mass quantification of the coated based CN materials was attempted before and after this washing; however, no mass variation was detected. This could be due to some fibers releasing on the edges of the fabrics during the washing step.

### 2.3. Catalyst characterization

X-ray diffraction (XRD) analysis was carried out in a PANalytical X'Pert MPD equipped with an X'Celerator detector and secondary monochromator (Cu K $\alpha$   $\lambda = 0.154\ \text{nm}$ , 50 kV, 40 mA; data recorded at a 0.017° step size, 100 s/step).

The optical absorption of the coated-CN cotton fabrics was followed by diffuse reflectance UV-Vis (DRUV-Vis) spectroscopy using a JASCO

V-560 spectrophotometer equipped with an integrating sphere.

Photoluminescence (PL) measurements of the coated fabrics were conducted at room temperature on a JASCO (FP 82000) fluorescence spectrometer with a 150 W Xenon lamp as light source, using bandwidths of 2.5 nm for emission and excitation.

Attenuated total reflectance (ATR) measurements ( $4000\text{--}600\ \text{cm}^{-1}$ ) were carried out in a JASCO FT/IR-6800 spectrometer (JASCO Analytical Instruments, USA), equipped with a MIRacle™ Single Reflection (ZnSe crystal plate; PIKE Technologies, USA).

X-ray photoelectron spectroscopy (XPS) was performed in a Kratos AXIS Ultra HSA, with CasaXPS software for data analysis. The analysis was carried out with a monochromatic Al K $\alpha$  X-ray source (1486.7 eV), operating at 15 kV (90 W), in FAT (Fixed Analyser Transmission) mode, with a pass energy of 40 eV for regions of interest and 80 eV for survey.

The morphology of the coated-fabrics was examined by scanning electron microscopy (SEM) using a FEI Quanta 400 FEG ESEM/EDAX Genesis X4M (15 keV) instrument.

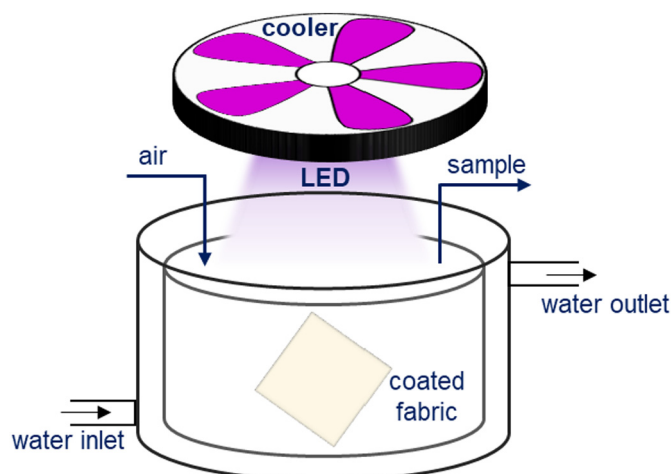
Conventional and high-resolution transmission electron microscopy (TEM/HRTEM) and atomically resolved scanning transmission electron microscopy (STEM) analyses of the colloidal CN was performed using a Cs probe-corrected TEM/STEM Jeol ARM 200 CF microscope equipped with a cold-FEG electron source, operated at 80 kV.

### 2.4. Photocatalytic experiments

The self-cleaning efficiency of the CN or GO/CN coated fabrics was assessed in the photocatalytic treatment of aqueous solutions containing caffeine or RhB (0.05 mM). In a typical photocatalytic experiment, a borosilicate reactor equipped with a water recirculation glass jacket (to maintain a constant temperature) was filled with 100 mL of the contaminant solution (Scheme 1). Then, a coated cotton fabric (6.0 cm  $\times$  6.0 cm) was placed inside the reactor and the contaminant solution was continuously supplied with air.

Before the photocatalytic experiments, dark reactions were performed to establish the adsorption-desorption equilibrium between the coated cotton fabrics and the contaminant for 60 min. In addition, the photochemical stability of both contaminants was also assessed under the same irradiation conditions, using uncoated fabric. The photocatalytic efficiency of the coated fabrics was evaluated for 360 min using a light emitting diode (LED) with a maximum wavelength at 417 nm. The intensity of the LED ( $115\ \text{W m}^{-2}$ ) was measured at 9 cm from the contaminant solution using an UV-Vis spectroradiometer apparatus (USB2000+, OceanOptics, USA).

During the photocatalytic experiments caffeine samples were regularly withdrawn from the reactor and analyzed by High Pressure Liquid Chromatography (HPLC) in a Hitachi Elite LaChrom apparatus,



Scheme 1. Setup used in the photocatalytic experiments.

equipped with a Diode Array Detector (L-2450) and using a Purospher Star RP-18 column (250 mm × 4.6 mm, 5 μm particles). The column was equilibrated with water:methanol (70:30) followed by a linear gradient run for 23 min. The caffeine concentration was determined at 274 nm. The RhB concentration was monitored by UV-Vis spectrophotometry using a Jasco V-560 spectrophotometer. Selected experiments were repeated in order to confirm the reproducibility of the results.

### 2.5. Photocatalytic *Escherichia coli* inactivation tests

Prior to the photocatalytic experiments, strain *Escherichia coli* (*E. coli*) DSM 1103 was cultured on Mueller-Hinton agar plates, at 30 °C overnight. Then, an *E. coli* suspension was prepared with sterile saline solution (0.85% w/v NaCl), in order to provide a cell density of ca.  $10^3$ – $10^4$  colony-forming units per milliliter (CFU mL<sup>-1</sup>) in each well of the microtiter plate used for the inactivation tests [27]. Moreover, each well comprised a total volume of 3 mL, made up of bacterial suspension, colloidal CN or GO/CN (~0.7 g L<sup>-1</sup>) and saline solution (in the case of control experiments). The photocatalytic reaction began once the irradiation was turned on (LED λ<sub>max</sub> = 417 nm; intensity = 17.2 W m<sup>-2</sup>; distance = 15.5 cm) and kept for 60 min. The samples were collected periodically and diluted in saline solution, prior to their spreading in Mueller-Hinton agar plates and incubation for 18 h at 37 °C. All the experiments were carried out in triplicate, at room temperature and under continuous stirring throughout the entire assay. Control experiments were conducted under dark conditions in order to evaluate the efficiency of the CN and GO/CN colloids in the absence of light.

## 3. Results and discussion

### 3.1. Characterization

The morphology of the coated fabrics was investigated by SEM, for comparison purposes, a SEM image of the control (uncoated fabric; Fig. 1a inset) is also shown. Fig. 1a and c exhibit a homogeneous distribution of the colloidal CN and GO/CN samples on the fabrics, respectively. SEM micrographs of the coated fabrics after several photocatalytic reaction cycles were also performed (Fig. 1b and d, using colloidal CN and GO/CN, respectively). The morphology of the coated fabrics was unchanged, indicative of their good stability under the applied experimental conditions. It is important to refer that the coated fabrics were washed with an anionic detergent between each reaction run using a water bath orbital shaker for 5 h at 70 °C. During this cleaning step, the water was regularly replaced by fresh one. Concerning the HR-TEM analysis, micrographs of the colloidal CN suggest the presence of thin nanosheets (Fig. 1e), where some porosity can also be observed, which may indicate the presence of defects on the CN surface. A more compact structure was observed in case of the powder CN (Fig. SD1), suggesting that the sonication treatment to obtain the colloidal CN led to thinner layers. Moreover, the HR-TEM image (Fig. 1f) showed an interlayer distance of around 0.26 nm. Due to the small content of GO (0.1% v/v) in the colloidal GO/CN sample, no changes were detected by HR-TEM (not shown), comparatively to the neat colloidal CN. Furthermore, the morphology similarity between both materials makes it difficult to differentiate between them.

The XDR diffraction pattern of CN powder synthesized by thermal decomposition of DCN is displayed in Fig. 2. The characteristic peaks of g-C<sub>3</sub>N<sub>4</sub> materials can be observed, and the stacking distance between layers was calculated by Bragg's law. The diffraction peak at 2θ = 12.97° observed in the pattern of CN powder corresponds to two adjacent planes with a distance of 0.68 nm. This peak is reported as the (100) plane, usually attributed to the in-plane repeating of the structural tri-s-triazine units [28]. Some studies demonstrated that the application of ultrasonication is a common method to break up agglomeration of nanoparticles, promoting their dispersion into stable colloids

[29,30]. In fact, concerning the colloidal CN the Tyndall effect was detected (Fig. SD2), suggesting the layers separation/break. Thus, the non-detected (100) plane in colloidal CN seems to indicate modifications between the tri-s-triazine structure units after the sonication treatment, which can be ascribed to the fragmentation of the ordering in-plane tri-s-triazine units observed before sonication (CN powder; Fig. 2).

The (002) crystal face corresponding to stacking of the conjugated aromatic network [31] was located at 2θ = 27.59° for powder and colloidal CN samples [31]. The interlayer staking distance calculated from the (002) peak was found similar for both CN samples (0.31 nm). These investigations correlate with the results observed by HR-TEM, in which a slight difference of the interlayer stacking distance between layers corresponding to the (002) plane was observed (0.26 nm).

The DRUV-Vis and PL measurements of the CN coated fabrics were assessed before the photocatalytic experiments and between each run, and the results were compared with the control fabric (Fig. 3). These analyses were performed in different points of the fabrics to prove the coating homogeneity. It was found that the optical properties of the coated fabrics remained constant after three cycles, with washings between them, suggesting their good stability.

To investigate the occurrence of electron-hole charge separation and transfer upon light excitation, PL measurements were performed and recorded upon an excitation with an energy of 3.35 eV (370 nm) at room temperature. As shown in Fig. 3b, the CN coated fabrics presented the characteristic pattern of a g-C<sub>3</sub>N<sub>4</sub> semiconductor [21], with an intense broad band located at ~435 nm, typically ascribed to the electron-hole recombination. Moreover, a weaker fluorescence emission band at ~525 nm was observed, which is commonly related with defects on the g-C<sub>3</sub>N<sub>4</sub> surface [14,20]. Comparing these results with the PL of the powder CN obtained on a previous work [21] (main broad band at ~441 nm), the coated fabrics showed a slight blue shift of ~6 nm. This observation can be presumably attributed to the quantum confinement effect due to the thinner layers of the material coated on the fabrics, which was already confirmed by HR-TEM. Moreover, the PL of the functional fabrics revealed a narrowing of the main broad band at ~441 nm comparatively to the original CN powder, suggesting intimate contact between the colloidal CN and cotton fabrics. This further attests the existence of a strong interaction between the colloidal CN with the fabric surface. Concerning the GO/CN coated fabrics, the quenching of the luminescence intensity was observed, which could indicate that, even at low percentages, GO acts as scavenger for photogenerated electrons generated on CN upon photoexcitation.

The chemical structure of the coated fabrics was analyzed by ATR. For comparison, the controls (powder CN and uncoated fabric) were also characterized (Fig. 4). As shown, the powder CN presents sharp peaks at ca. 805 cm<sup>-1</sup>, being ascribed to the tri-s-triazine ring units, and a broad band from the 3000 to 3500 cm<sup>-1</sup> range, which is commonly attributed to primary and secondary amines such as -NH<sub>2</sub> or N-H groups [20]. This band is also associated to the stretching of hydroxyl groups (O-H) of adsorbed water molecules. In case of the uncoated fabric, a broad band arising at 3000–3700 cm<sup>-1</sup> is assigned to O-H bonds that can be related to adsorbed water on the cotton surface, as well as to the characteristic O-H functional groups existing in cellulose (cotton fabric) [5,32]. A weak broad band around 2900 cm<sup>-1</sup>, corresponding to O-H stretching, is also observed. Moreover, vibrations in the 800–1500 cm<sup>-1</sup> range can be noticed, that are associated to the C-H, O-H, C-O and C-O-C bonds, characteristic of cellulose [5]. Concerning the coated fabrics, similar patterns are observed with additional peaks at 805 cm<sup>-1</sup>, confirming the tri-s-triazine ring structure on the coated fabrics. The non-detected stretching of the N-H groups in the 2800 to 3500 cm<sup>-1</sup> range in the coated fabrics may indicate that these groups are involved in the interactions between the nanomaterials and the cotton.

The surface chemistry colloidal CN sample was investigated by XPS analysis (Fig. 5) and compared with the powder CN sample (*i.e.*, before

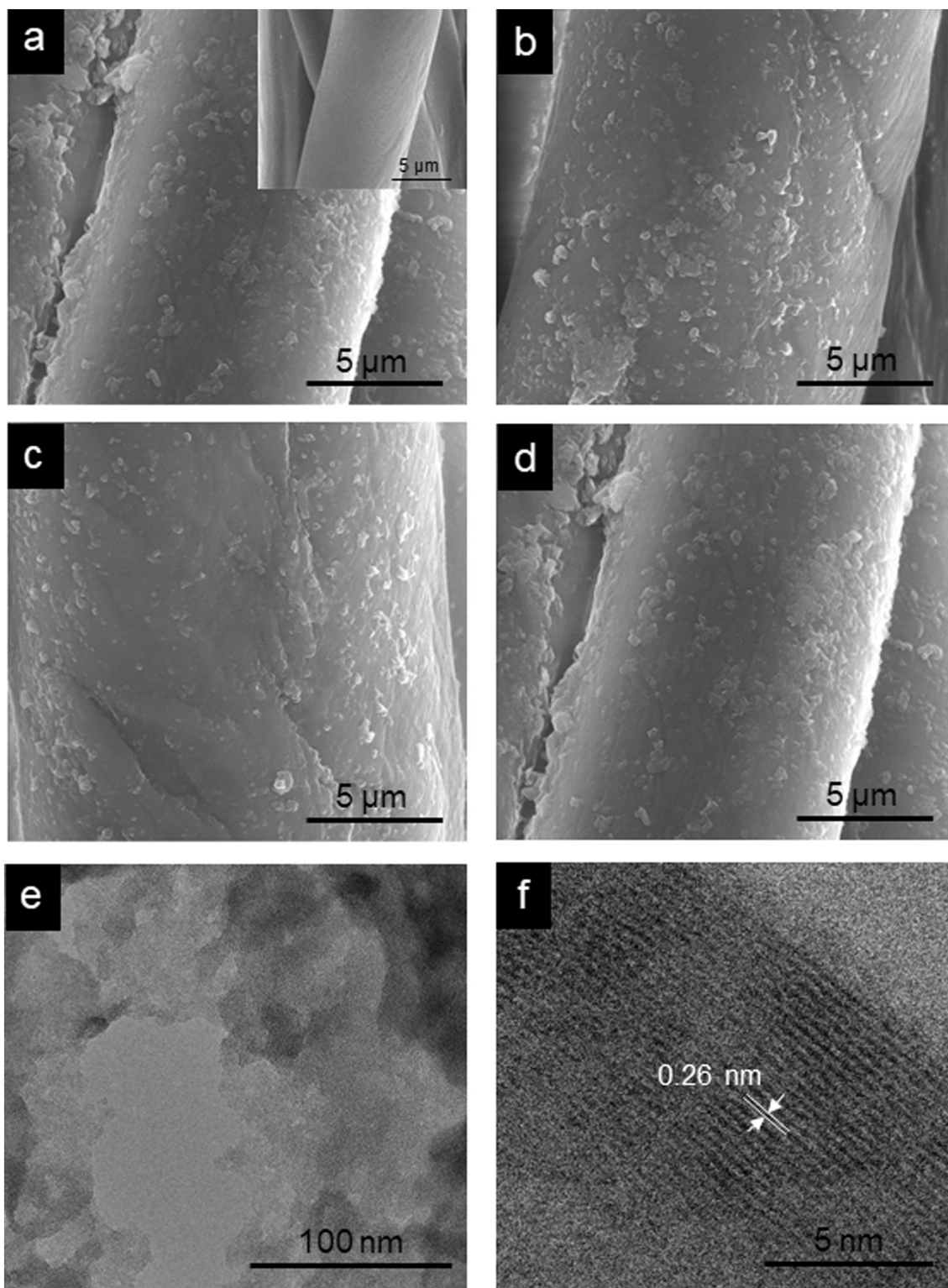


Fig. 1. SEM micrographs of CN and GO/CN coated fabrics before (a and c) and after (b and d) 3 reuse cycles, respectively. HR-TEM of the colloidal CN (e and f).

the ultrasonication treatment). The N1s region of each material (Fig. 5a and b) was deconvoluted into four peaks at 398.9, 399.6, 401.3 and 405.0 eV. As reported in a previous work [21], the CN powder exhibited a peak at 398.9 eV that can be assigned to  $sp^2$  hybridized N in triazine rings (C=N-C). Moreover, the peak with a binding energy of 399.7 eV may reflect the occurrence of tertiary N in N-(C<sub>3</sub>) or H-N-(C<sub>2</sub>) units, the residual amino functional groups (C-NH<sub>x</sub>) can be confirmed at 401.3 eV, and the peak at 405.0 eV is commonly allocated to -NO<sub>2</sub>

terminal groups [21,33,34]. In the case of colloidal CN, analogous peaks in the N1s region were observed, yet the atomic percentages of N1s regions showed variations, suggesting some modifications on the surface chemistry of the material. These deviations can be attributed to different contents of O species on the CN colloidal surface, as shown in Fig. 5c and d. In the O1s region, a shift to higher energies (533.06 eV) compared to the powder CN material (532.9 eV) for colloidal CN was observed (Fig. 5c and d, respectively), indicating the presence of

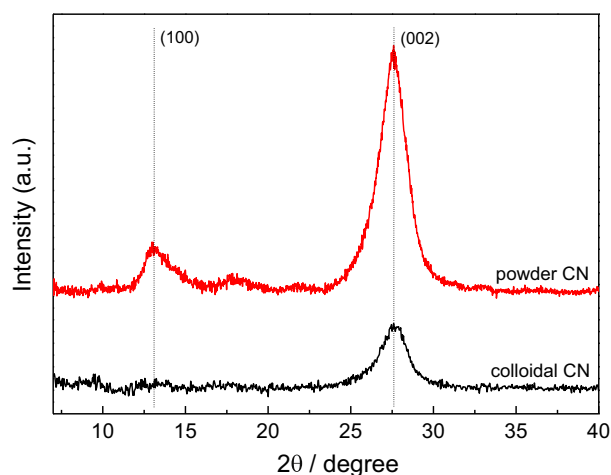


Fig. 2. X-ray diffraction analysis of powder and colloidal CN samples.

adsorbed water molecules. Furthermore, the second peak at 531.4 eV may indicate the formation of  $-OH$  surface groups [33]. This distinct profile of the colloidal CN material could be ascribed to the post-treatment, more precisely to the exposure of the colloidal CN to the high intensity sonication that can eventually break the CN structure, thus, suggesting a substitution by  $-O$  and/or  $-OH$  groups, which can act as the cross-linker forming C-O-C bonds with the cellulose (cotton). The deconvolution of the C1s peak of powder CN catalyst revealed three components centered at 285.0, 286.1 and 288.6 eV (Fig. 5e), commonly attributed to  $C(-N)_3$ ,  $C-NH_2$  and  $N-C=N$  groups, respectively [20,21]. The main peak at 288.6 eV of the powder CN confirmed the presence of  $sp^3$ -bonded defects on the CN surface. An additional peak at 287.2 eV was observed on the colloidal CN (Fig. 5f), suggesting the presence of C-O bonds [35,36], corroborated with the O1s peak observed for colloidal CN sample. These observations are indicative of the presence of additional bonds that can be responsible for the chemical changes of the colloidal CN, which may enhance the contact between this material and the cotton fabric.

### 3.2. Photocatalytic self-cleaning of the coated fabrics

To evaluate the photocatalytic self-cleaning properties of the CN and GO/CN coatings, a small piece of coated fabric was placed in contact with aqueous solutions of caffeine and RhB (models used as organic contaminants). Owing the activity of CN-based materials under

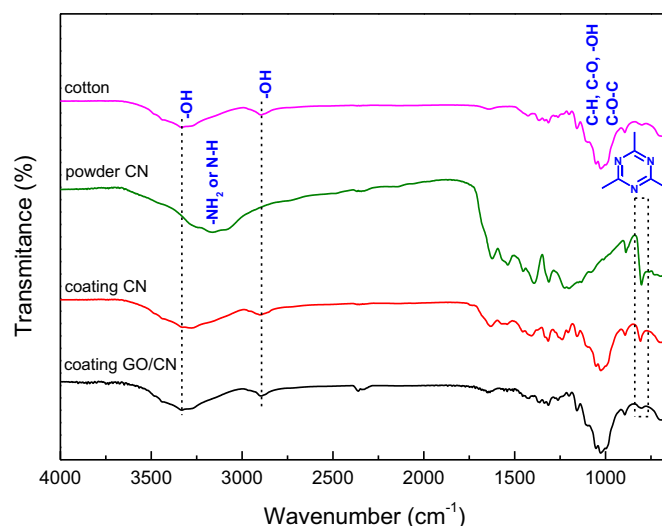


Fig. 4. ATR of CN-based coated fabrics comparing with the controls (powder CN and uncoated cotton fabric).

visible light, the photocatalytic experiments were conducted using a LED system ( $\lambda_{max} = 417$  nm) for 360 min. Prior to irradiation, adsorption-desorption experiments using the coated fabrics were performed for 60 min, negligible adsorption of the contaminants on the coated fabrics being observed (as observed in Fig. 6c for RhB and  $t < 0$  min). In addition, the photochemical stability of the organic contaminants under LED irradiation was evaluated. As expected, both molecules revealed to be stable, since the maximum absorbance of caffeine and RhB is 278 nm and 564 nm, respectively. Moreover, photocatalytic experiments using uncoated fabrics showed no activity for the degradation of caffeine or RhB (Fig. SD3). The photocatalytic reactions followed a pseudo first-order kinetics, as displayed in Fig. 6. In the presence of the CN coated fabric, a remarkable degradation of the target contaminants was obtained after 360 min. The coated GO/CN fabric showed higher efficiency for the degradation of both caffeine and RhB, compared with the coated CN fabric. The improved activity of optical semiconductors promoted by the presence of GO has been extensively reported in the literature [6,37–39]. This activity enhancement can be attributed to distinct factors, including: i) increased catalyst surface area; ii) oxidized carbon structures promoting the optical semiconductor dispersion; iii) photosensitization of optical semiconductors by carbon materials; and iv) carbon materials acting as co-adsorbents. Several works reported that the surface area can

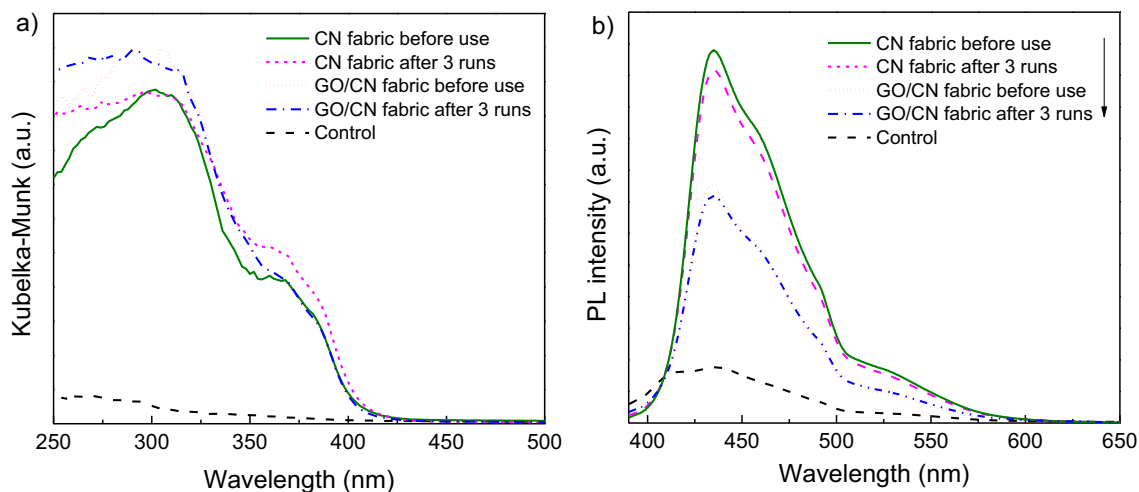


Fig. 3. DRUV-Vis (a) and PL (b) analyses of uncoated fabric (control) and coated fabrics.

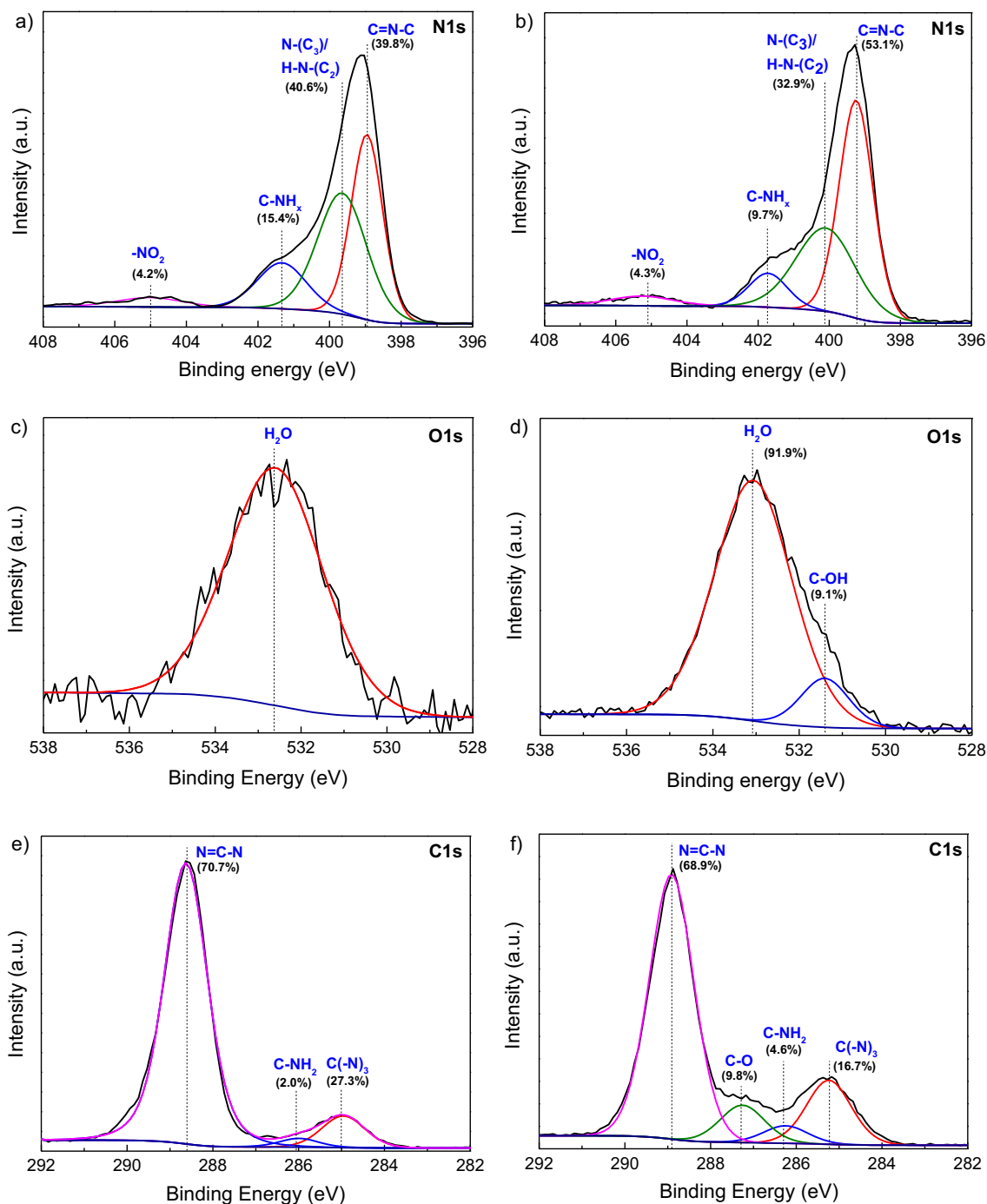


Fig. 5. XPS spectra (N1s, O1s and C1s) of powder and colloidal CN (a, c and e; b, d and f, respectively).

significantly enhance the efficiency of the resulting materials. Yet, this hypothesis can be discarded in the present work, due to a variety of reasons. Firstly, the used GO exhibits a low surface area ( $\sim 5 \text{ m}^2 \text{ g}^{-1}$ ) [26], and the small percentage used in the preparation of the hybrid material is unable to enhance the surface area of the resulting material.

A notorious quenching of the PL intensity of the GO/CN coated fabric was observed. This may indicate that the presence of GO prevents the recombination of the photogenerated electron-hole pairs upon photo-excitation, leading to a faster degradation of the contaminants. Due to the high hydrophilicity of cotton, systems involving aqueous media improve the transport of active reagents between the cotton fabrics [40]. Thus, the cotton hydrophilic capacity may also contribute to the large extent of functionalization using aqueous colloidal CN-

based materials. Moreover, the subsequent contact between the photoactivated surfaces and the target contaminants can also be improved. When the fabrics were placed in contact with RhB under dark conditions, the effective dyeing of cotton was observed, yet < 5% of RhB adsorption was found after 60 min (Fig. 6c). After the photocatalytic reactions, it can be observed that the coated fabric returns to its natural color, showing total RhB removal, as displayed on the absorption spectrum (Fig. 6c; inset). It is also important to refer that after the coating with CN-based materials negligible changes of the natural cotton color were observed; however, based on the electronic and optical properties measurements of the coated fabrics, the presence of the photocatalysts was confirmed.

To evaluate the effect of GO phase in the photocatalytic degradation

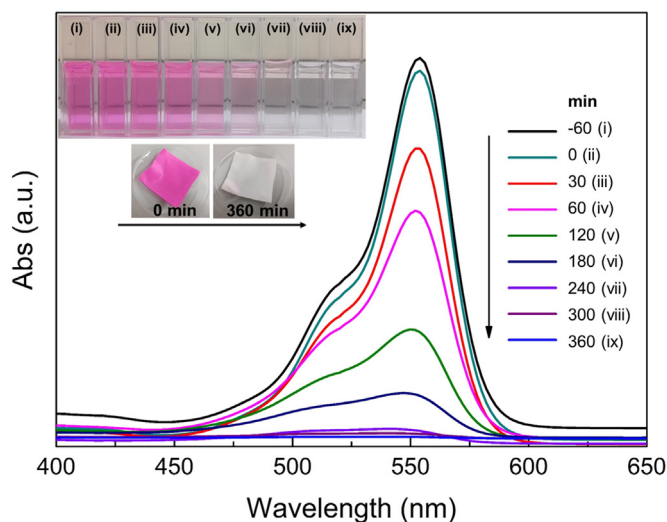


Fig. 6. Photocatalytic degradation of caffeine (a) and RhB (b) using the CN and GO/CN coated fabrics. Selected experiment showing the absorption spectra of RhB abatement in presence of the GO/CN coated fabrics under visible light irradiation (c).

of the contaminants, experiments using fabrics coated with 0.1% v/v of GO were performed under dark and light irradiation conditions (not shown). The coating of the fabrics (with 0.1% v/v GO) was carried out under the same experimental conditions. From these experiments no degradation of the contaminants was found, suggesting that the efficiency of the GO/CN coated fabrics results from cooperative interactions between both materials.

To evaluate the stability of the coated surfaces, reutilization experiments (using both materials) were conducted, maintaining the operational conditions used in the previously described photocatalytic reactions. As mentioned above, the coated surfaces were thoroughly washed between each run. As displayed in Fig. 7, the efficiencies of both coated surfaces remained practically constant after three runs, suggesting good stability under the photocatalytic conditions.

Regarding the photocatalytic self-cleaning results of the coated textiles, it seems that the high efficiency of the coated GO/CN sample compared with the coated CN material can be attributed to the facilitated electron transfer from CN to GO. When the GO/CN coated fabric is exposed to light, GO can act as an electron scavenger for the photoexcited CN, delaying the recombination of electron-hole pairs.

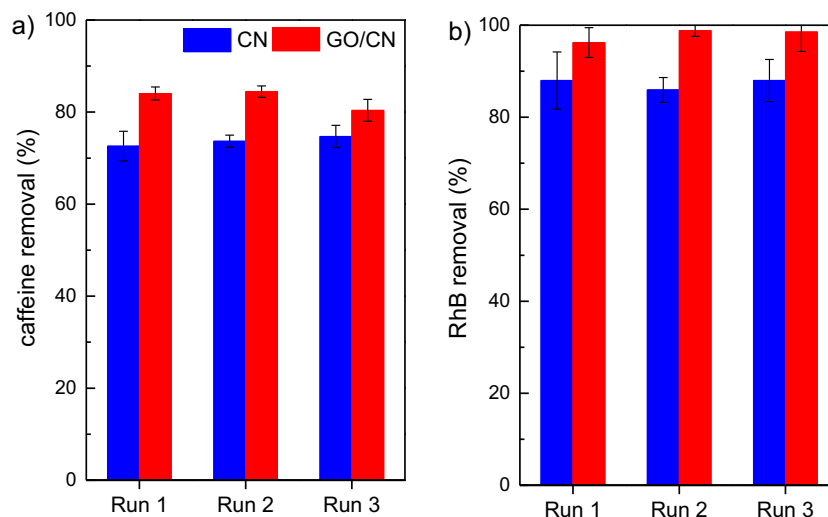


Fig. 7. Reusability assessment for the coated fabrics in the degradation of caffeine (a) and RhB (b) after 240 min reaction.

Recently, Fan *et al.* reported that a cotton fabric treated with  $\text{gC}_3\text{N}_4$  provided ca. 75% of RhB degradation within 60 min under simulated sunlight [5]. Nevertheless, the authors used a lower concentration of RhB ( $10 \text{ mg L}^{-1}$ ) and a Xenon lamp with a wider wavelength interval (350–780 nm), while a RhB concentration ( $24 \text{ mg L}^{-1}$ ) larger than twice was employed in the current study with a cost-effective and energy-efficient visible LED, with a maximum emission wavelength at 417 nm.

### 3.3. Photocatalytic inactivation of neat CN and GO/CN colloids against *E. coli*

Bacterial inactivation (initial concentration of  $10^3 - 10^4 \text{ CFU mL}^{-1}$ ) was ca. 99.9 and 99.2% after 60 min with  $0.7 \text{ g L}^{-1}$  CN and GO/CN colloids, under  $17.2 \text{ W m}^{-2}$  of LED light intensity, respectively (Fig. 8). Sun *et al.* [6], reported around 50% of *E. coli* inactivation (initial concentration of  $10^7 \text{ CFU mL}^{-1}$ ) with a  $0.1 \text{ g L}^{-1}$  of a GO/ $\text{gC}_3\text{N}_4$  composite under visible irradiation (Xenon lamp with a cut-off filter of  $\lambda > 420 \text{ nm}$  and an intensity of  $3000 \text{ W m}^{-2}$ ), has been reported after 60 min. These authors documented that the light-induced holes were the main reactive species for *E. coli* inactivation with the composite material. This was further confirmed by Huang *et al.* [41] which also suggested that light-induced holes on the surface of  $\text{g-C}_3\text{N}_4$  were predominant in the oxidative pathway of *E. coli* inactivation by photocatalysis. Therefore, a parallel to the present work can be drawn, given that a similar photocatalyst and visible light activation occurred in both situations. Bacterial inactivation processes can implicate alterations in the microorganism cell integrity and shape [42]. Possibly, abnormal cell shapes began to occur during photocatalysis with  $\text{gC}_3\text{N}_4$ , followed by cell wall rupture [43], facilitating the entrance of reactive species in the cell and also the leakage of cytoplasm and cell organelles [44].

Overall, a few factors like, light intensity, catalyst concentration and initial bacterial concentration need to be taken into consideration in this type of studies. Special attention should be paid to the economical factor associated with the use of higher light intensities for this type of applications, cost-effective and energy-efficient LEDs being a promising option in comparison with other artificial lamps.

## 4. Conclusions

Neat CN and a GO/CN hybrid materials were successfully coated on cotton textiles. High photocatalytic self-cleaning activity was achieved, using caffeine and RhB as target contaminants under visible light irradiation. Among the coated textiles tested, the fabric containing the GO/

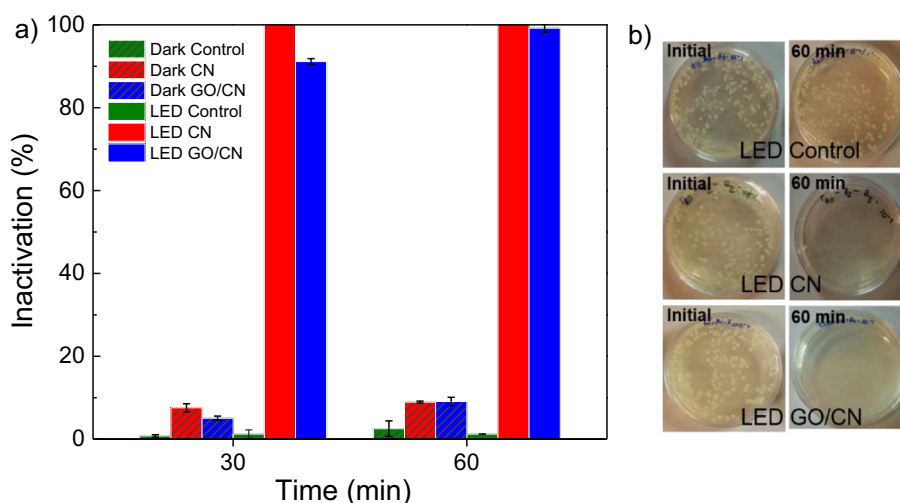


**Fig. 8.** *E. coli* inactivation with CN and GO/CN colloids and control experiments, under visible light (LED) and dark conditions (Dark) (a); and the incubated agar plates inoculated with bacterial suspension and colloids or control before and after 60 min of LED irradiation (b).

CN hybrid showed the highest performance, achieving almost complete degradation of caffeine and RhB after 360 min. The reutilization experiments proved that both coated CN and coated GO/CN hybrid fabrics hold excellent stability under the reaction conditions used. Taking this in consideration, together with the characterization of the coated fabrics, the results suggest that an effective attachment between the cotton and the photocatalysts is attained. Bacterial inactivation of > 99.2% was obtained with CN-based colloids activated by LED light, suggesting disinfection potentialities. Thus, functional textiles proposed here eliminate the need for frequent washing, as they are effective, the carbon phase allowing degradation of organic molecules that can stain the fabric. In addition, the CN-based colloids presented high performance in the inactivation of a common potentially pathogenic microorganism.

### Acknowledgments

This work was financially supported by Project POCI-01-0145-FEDER-030674 funded by ERDF through COMPETE2020 - Programa Operacional Competitividade e Internacionalização (POCI) – and by national funds through FCT - Fundação para a Ciência e a Tecnologia. We would also like to thank the scientific collaboration under project “AIProcMat@N2020 – Advanced Industrial Processes and Materials for a Sustainable Northern Region of Portugal 2020” (NORTE-01-0145-FEDER-000006; NORTE 2020 - Portugal 2020 Partnership Agreement, through FEDER) and project Associate Laboratory LSRE-LCM - UID/EQU/50020/2019 - funded by national funds through FCT/MCTES (PIDDAC). M.P. gratefully acknowledges FCT for her scholarship SFRH/BD/102086/2014. C.G.S. acknowledges the FCT Investigator Programme (IF/00514/2014) with financing from the European Social Fund (ESF) and the Human Potential Operational Programme. We thank CeNTI (Portugal) for supplying the fabrics. We are indebted to Dr. Carlos Sá and the CEMUP team (Portugal) for technical assistance and advice with SEM measurements.

### Appendix A. Supplementary data

Supplementary data to this article can be found online at <https://doi.org/10.1016/j.apsusc.2019.143757>.

### References

- [1] R. Nosrati, A. Olad, S. Shakoobi, Preparation of an antibacterial, hydrophilic and photocatalytically active polyacrylic coating using TiO<sub>2</sub> nanoparticles sensitized by graphene oxide, *Mater. Sci. Eng. C* 80 (2017) 642–651.
- [2] M. Zahid, E.L. Papadopoulou, G. Suarato, V.D. Binas, G. Kiriakidis, I. Gounaki, O. Moira, D. Venieri, I.S. Bayer, A. Athanassiou, Fabrication of visible light-induced antibacterial and self-cleaning cotton fabrics using manganese doped TiO<sub>2</sub> nanoparticles, *ACS Appl. Bio Mater.* 1 (2018) 1154–1164.
- [3] M. Abid, S. Bouattour, A.M. Ferrara, D.S. Conceição, A.P. Carapeto, L.F. Vieira Ferreira, A.M. Botelho do Rego, M.M. Chehimi, M. Rei Vilar, S. Boufi, Facile functionalization of cotton with nanostructured silver/titanium for visible-light plasmonic photocatalysis, *J. Colloid Interface Sci.* 507 (2017) 83–94.
- [4] J. Hu, Q. Gao, L. Xu, M. Wang, M. Zhang, K. Zhang, W. Liu, G. Wu, Functionalization of cotton fabrics with highly durable polysiloxane–TiO<sub>2</sub> hybrid layers: potential applications for photo-induced water–oil separation, UV shielding, and self-cleaning, *J. Mater. Chem. A* 6 (2018) 6085–6095.
- [5] Y. Fan, J. Zhou, J. Zhang, Y. Lou, Z. Huang, Y. Ye, L. Jia, B. Tang, Photocatalysis and self-cleaning from g-C<sub>3</sub>N<sub>4</sub> coated cotton fabrics under sunlight irradiation, *Chem. Phys. Lett.* 699 (2018) 146–154.
- [6] L. Sun, T. Du, C. Hu, J. Chen, J. Lu, Z. Lu, H. Han, Antibacterial activity of graphene oxide/g-C<sub>3</sub>N<sub>4</sub> composite through photocatalytic disinfection under visible light, *ACS Sustain. Chem. Eng.* 5 (2017) 8693–8701.
- [7] N. Bouazizi, A. El achari, C. Campagne, J. Vieillard, A. Azzouz, Copper oxide coated polyester fabrics with enhanced catalytic properties towards the reduction of 4-nitrophenol, *J. Mater. Sci. Mater. Electron.* 29 (2018) 10802–10813.
- [8] W.-D. Li, J. Gao, L. Wang, Enhancement of durable photocatalytic properties of cotton/polyester fabrics using TiO<sub>2</sub>/SiO<sub>2</sub> via one step sonosynthesis, *J. Ind. Text.* 46 (2016) 1633–1655.
- [9] D. Cheng, M. He, J. Ran, G. Cai, J. Wu, X. Wang, In situ reduction of TiO<sub>2</sub> nanoparticles on cotton fabrics through polydopamine templates for photocatalysis and UV protection, *Cellulose* 25 (2018) 1413–1424.
- [10] M. Shaban, S. Abdallah, A.A. Khalek, Characterization and photocatalytic properties of cotton fibers modified with ZnO nanoparticles using sol–gel spin coating technique, *Beni-Suef Univ. J. Basic Appl. Sci.* 5 (2016) 277–283.
- [11] H.H. Lara, E.N. Garza-Treviño, L. Ixtepan-Turrent, D.K. Singh, Silver nanoparticles are broad-spectrum bactericidal and virucidal compounds, *J. Nanobiotechnol.* 9 (2011) 30.
- [12] A.K. Yetisen, H. Qu, A. Manbachi, H. Butt, M.R. Dokmeci, J.P. Hinestroza, M. Skorobogatiy, A. Khademhosseini, S.H. Yun, Nanotechnology in textiles, *ACS Nano* 10 (2016) 3042–3068.
- [13] R. Borda d’Água, R. Branquinho, M.P. Duarte, E. Maurício, A.L. Fernando, R. Martins, E. Fortunato, Efficient coverage of ZnO nanoparticles on cotton fibres for antibacterial finishing using a rapid and low cost in situ synthesis, *New J. Chem.* 42 (2018) 1052–1060.
- [14] M.J. Sampaio, M.J. Lima, D.L. Baptista, A.M.T. Silva, C.G. Silva, J.L. Faria, Ag-loaded ZnO materials for photocatalytic water treatment, *Chem. Eng. J.* 318 (2017) 95–102.
- [15] R. Salomoni, P. Léo, A.F. Montemor, B.G. Rinaldi, M. Rodrigues, Antibacterial effect of silver nanoparticles in *Pseudomonas aeruginosa*, *Nanotechnol. Sci. Appl.* 10 (2017) 115–121.
- [16] A. Panacek, R. Prucek, D. Safarova, M. Dittrich, J. Richtrova, K. Benickova, R. Zboril, L. Kvitek, Acute and chronic toxicity effects of silver nanoparticles (NPs) on *Drosophila melanogaster*, *Environ. Sci. Technol.* 45 (2011) 4974–4979.
- [17] T. Matsunaga, M. Okochi, TiO<sub>2</sub>-mediated photochemical disinfection of *Escherichia coli* using optical fibers, *Environ. Sci. Technol.* 29 (1995) 501–505.
- [18] A. Kubacka, M.S. Diez, D. Rojo, R. Bargiela, S. Giordina, I. Zapico, J.P. Albar, C. Barbas, V.A.P. Martins dos Santos, M. Fernández-García, M. Ferrer, Understanding the antimicrobial mechanism of TiO<sub>2</sub>-based nanocomposite films in a pathogenic bacterium, *Sci. Rep.* 4 (2014) 4134.
- [19] S. Landi, J. Carneiro, S. Ferdov, A.M. Fonseca, I.C. Neves, M. Ferreira, P. Parpot,

- O.S.G.P. Soares, M.F.R. Pereira, Photocatalytic degradation of rhodamine B dye by cotton textile coated with SiO<sub>2</sub>-TiO<sub>2</sub> and SiO<sub>2</sub>-TiO<sub>2</sub>-HY composites, *J. Photochem. Photobiol. A Chem.* 346 (2017) 60–69.
- [20] E.S. Da Silva, N.M.M. Moura, A. Coutinho, G. Dražić, B.M.S. Teixeira, N.A. Sobolev, C.G. Silva, M.G.P.M.S. Neves, M. Prieto, J.L. Faria,  $\beta$ -Cyclodextrin as a precursor to holey C-doped g-C<sub>3</sub>N<sub>4</sub> nanosheets for photocatalytic hydrogen generation, *ChemSusChem*, 11 (2018) 2681–2694.
- [21] M.J. Lima, A.M.T. Silva, C.G. Silva, J.L. Faria, Graphitic carbon nitride modified by thermal, chemical and mechanical processes as metal-free photocatalyst for the selective synthesis of benzaldehyde from benzyl alcohol, *J. Catal.* 353 (2017) 44–53.
- [22] A. Naseri, M. Samadi, A. Pourjavadi, A.Z. Moshfegh, S. Ramakrishna, Graphitic carbon nitride (g-C<sub>3</sub>N<sub>4</sub>)-based photocatalysts for solar hydrogen generation: recent advances and future development directions, *J. Mater. Chem. A* 5 (2017) 23406–23433.
- [23] D.A. Giannakoudakis, Y. Hu, M. Florent, T.J. Bandosz, Smart textiles of MOF/g-C<sub>3</sub>N<sub>4</sub> nanospheres for the rapid detection/detoxification of chemical warfare agents, *Nanoscale Horizons* 2 (2017) 356–364.
- [24] Y. Wang, X. Ding, P. Zhang, Q. Wang, K. Zheng, L. Chen, J. Ding, X. Tian, X. Zhang, Convenient and recyclable TiO<sub>2</sub>/g-C<sub>3</sub>N<sub>4</sub> photocatalytic coating: layer-by-layer self-assembly construction on cotton fabrics leading to improved catalytic activity under visible light, *Ind. Eng. Chem. Res.* (2019).
- [25] M.J. Lima, P.B. Tavares, A.M.T. Silva, C.G. Silva, J.L. Faria, Selective photocatalytic oxidation of benzyl alcohol to benzaldehyde by using metal-loaded g-C<sub>3</sub>N<sub>4</sub> photocatalysts, *Catal. Today* 287 (2017) 70–77.
- [26] M. Pedrosa, L.M. Pastrana-Martínez, M.F.R. Pereira, J.L. Faria, J.L. Figueiredo, A.M.T. Silva, N/S-doped graphene derivatives and TiO<sub>2</sub> for catalytic ozonation and photocatalysis of water pollutants, *Chem. Eng. J.* 348 (2018) 888–897.
- [27] R.A.R. Monteiro, S.M. Miranda, V.J.P. Vilar, L.M. Pastrana-Martínez, P.B. Tavares, R.A.R. Boaventura, J.L. Faria, E. Pinto, A.M.T. Silva, N-modified TiO<sub>2</sub> photocatalytic activity towards diphenhydramine degradation and *Escherichia coli* inactivation in aqueous solutions, *Appl. Catal. B Environ.* 162 (2015) 66–74.
- [28] A. Hatamie, F. Marahel, A. Sharifat, Green synthesis of graphitic carbon nitride nanosheet (g-C<sub>3</sub>N<sub>4</sub>) and using it as a label-free fluorosensor for detection of metronidazole via quenching of the fluorescence, *Talanta* 176 (2018) 518–525.
- [29] B. Ruan, A.M. Jacobi, Ultrasonication effects on thermal and rheological properties of carbon nanotube suspensions, *Nanoscale Res. Lett.* 7 (2012) 127.
- [30] I.M. Mahbubul, T.H. Chong, S.S. Khaleduzzaman, I.M. Shahrul, R. Saidur, B.D. Long, M.A. Amalina, Effect of ultrasonication duration on colloidal structure and viscosity of alumina–water nanofluid, *Ind. Eng. Chem. Res.* (16) (2014) 6677–6684.
- [31] X. Wang, K. Maeda, A. Thomas, K. Takanahe, G. Xin, J.M. Carlsson, K. Domen, M. Antonietti, A metal-free polymeric photocatalyst for hydrogen production from water under visible light, *Nat. Mater.* 8 (2008) 76.
- [32] S.S. Ugur, M. Sariisik, A.H. Aktas, The fabrication of nanocomposite thin films with TiO<sub>2</sub> nanoparticles by the layer-by-layer deposition method for multifunctional cotton fabrics, *Nanotechnology* 21 (2010) 325603.
- [33] Z. Zhao, Y. Sun, Q. Luo, F. Dong, H. Li, W.-K. Ho, Mass-controlled direct synthesis of graphene-like carbon nitride nanosheets with exceptional high visible light activity. Less is better, *Sci. Rep.* 5 (2015) 14643.
- [34] I. Papailias, N. Todorova, T. Giannakopoulou, N. Ioannidis, N. Boukos, C.P. Athanasekou, D. Dimotikali, C. Trapalis, Chemical vs thermal exfoliation of g-C<sub>3</sub>N<sub>4</sub> for NO<sub>x</sub> removal under visible light irradiation, *Appl. Catal. B Environ.* 239 (2018) 16–26.
- [35] H.S. Kim, Y.H. Kim, K.C. Roh, K.-B. Kim, Sandwich-type ordered mesoporous carbon/graphene nanocomposites derived from ionic liquid, *Nano Res.* 9 (2016) 2696–2706.
- [36] W. Wang, J.C. Yu, D. Xia, P.K. Wong, Y. Li, Graphene and g-C<sub>3</sub>N<sub>4</sub> nanosheets cowrapped elemental  $\alpha$ -sulfur as a novel metal-free heterojunction photocatalyst for bacterial inactivation under visible-light, *Environ. Sci. Technol.* 47 (2013) 8724–8732.
- [37] G. Liao, S. Chen, X. Quan, H. Yu, H. Zhao, Graphene oxide modified g-C<sub>3</sub>N<sub>4</sub> hybrid with enhanced photocatalytic capability under visible light irradiation, *J. Mater. Chem.* 22 (2012) 2721–2726.
- [38] M.J. Sampaio, R.R. Bacsá, A. Benyounes, R. Axet, P. Serp, C.G. Silva, A.M.T. Silva, J.L. Faria, Synergistic effect between carbon nanomaterials and ZnO for photocatalytic water decontamination, *J. Catal.* 331 (2015) 172–180.
- [39] H. Wang, Q. Shen, Z. You, Y. Su, Y. Yu, A. Babapour, F. Zhang, D. Cheng, H. Yang, Preparation of nanoscale-dispersed g-C<sub>3</sub>N<sub>4</sub>/graphene oxide composite photocatalyst with enhanced visible-light photocatalytic activity, *Mater. Lett.* 217 (2018) 143–145.
- [40] T. Topalovic, V.A. Nierstrasz, L. Bautista, D. Jocić, A. Navarro, M.M.C.G. Warmoeskerken, XPS and contact angle study of cotton surface oxidation by catalytic bleaching, *Colloids Surf. A Physicochem. Eng. Asp.* 296 (2007) 76–85.
- [41] J. Huang, W. Ho, X. Wang, Metal-free disinfection effects induced by graphitic carbon nitride polymers under visible light illumination, *Chem. Commun.* 50 (2014) 4338–4340.
- [42] C. Zhang, Y. Li, D. Shuai, Y. Shen, W. Xiong, L. Wang, Graphitic carbon nitride (g-C<sub>3</sub>N<sub>4</sub>)-based photocatalysts for water disinfection and microbial control: a review, *Chemosphere* 214 (2019) 462–479.
- [43] H. Zhao, H. Yu, X. Quan, S. Chen, Y. Zhang, H. Zhao, H. Wang, Fabrication of atomic single layer graphitic-C<sub>3</sub>N<sub>4</sub> and its high performance of photocatalytic disinfection under visible light irradiation, *Appl. Catal. B Environ.* 152–153 (2014) 46–50.
- [44] J. Deng, J. Liang, M. Li, M. Tong, Enhanced visible-light-driven photocatalytic bacteria disinfection by g-C<sub>3</sub>N<sub>4</sub>-AgBr, *Colloids Surf. B: Biointerfaces* 152 (2017) 49–57.